



Cite this: *Photochem. Photobiol. Sci.*, 2018, **17**, 622

## Enhanced phosphorescence properties of a Pt-porphyrin derivative fixed on the surface of nano-porous glass†

Toshiko Mizokuro,<sup>a</sup> Aizitaili Abulikemu,<sup>b</sup> Yusuke Sakagami,<sup>b,c</sup> Tetsuro Jin<sup>b</sup> and Kenji Kamada<sup>b,c</sup>

The room-temperature phosphorescence chromophore, Pt(II) coproporphyrin I (PtCP), was fixed on the surface of a 3D-network of nanoscale pores of porous glass through ion-exchange reaction. The absorption and phosphorescence spectra indicated that PtCP can be loaded while maintaining monomeric dispersion at concentrations well beyond solubility limits of PtCP in solution. The phosphorescence quantum yield of PtCP fixed on the surface was also found to have double the enhancement of solution. The extended lifetime of phosphorescence of PtCP bonded on the surface compared to that in solution clearly indicated that suppression of nonradiative deactivation plays a key role in high quantum yield and long triplet lifetime. This hybridization with nano-porous glass provides opportunities for various potential applications.

Received 14th December 2017,

Accepted 16th March 2018

DOI: 10.1039/c7pp00449d

rsc.li/ppps

## Introduction

Some chromophores like metalloporphyrins are known to show room-temperature (RT) phosphorescence, which has attracted considerable attention due to various applications such as oxygen<sup>1–4</sup> and pressure sensors,<sup>4,5</sup> organic light-emitting diodes (OLED),<sup>6–11</sup> and sensitizers for wavelength conversion devices<sup>12–17</sup> based on triplet-triplet annihilation upconversion (TTA-UC) utilising high triplet quantum yield. Solid materials are preferable for such device applications; however, many RT-phosphorescence chromophores easily aggregate<sup>18</sup> and cause phosphorescence quenching. Therefore, it is important to develop a method for achieving molecular-dispersed chromophores in the solid state at high concentration, retaining phosphorescence properties at the monomeric level.

One strategy to prevent aggregation is by fixing chromophores on the surface of a solid platform while maintaining molecular dispersion. Using a rigid fixing process, such as chemical bonding, each chromophore is bonded at a specific point of the solid surface while prohibiting their migration,

which prevents further aggregation on the surface. Moreover, by placing chromophores on the solid surface rather than in the bulk solid, the chromophores are exposed to free space that can be filled with the target matter, *i.e.* gases, liquids, or solids that can receive excitation energy from the chromophores for sensing and other purposes. Possible solid platforms include glass, oxides such as TiO<sub>2</sub>, and nano-sheet materials like clay. The luminescence properties of chromophores, especially porphyrins, hybridized with such materials have been studied extensively. For example, it was reported that porphyrin derivatives could be fixed on the surface of clay nano-sheets without aggregation and exhibited monomeric fluorescence.<sup>19</sup> Nano-sheet materials, however, are not suitable for the device applications mentioned above because they are contained in a dispersed solution or stacked as solids.

Nano-porous glass<sup>20</sup> is a material with unique properties. It has nm-scale pores connected to each other and forms a 3D-network of nano-pores, enabling an extremely large pore surface area per volume and a large free volume into which other materials like gases and fluids can penetrate. Nano-porous glass could be fabricated through phase-separation technology<sup>20</sup> from soda borosilicate glass capable of an average pore diameter of 30 nm or more. It was considered then that this material has potential for use as a solid platform for fixing chromophores.

In this work, we use nano-porous glass as a solid platform for fixing RT-phosphorescence chromophores and investigated the phosphorescence properties of chromophores bonded on the solid surface. For the chromophore, we chose Pt(II) copro-

<sup>a</sup>ESPRIT, National Institute of Advanced Industrial Science and Technology (AIST), 1-1-1 Higashi, Tsukuba, Ibaraki 305-8565, Japan. E-mail: chem42@ni.aist.go.jp

<sup>b</sup>IFMRI, National Institute of Advanced Industrial Science and Technology (AIST), 1-8-31 Midorigaoka, Ikeda, Osaka 563-8577, Japan. E-mail: k.kamada@aist.go.jp

<sup>c</sup>Department of Chemistry, School of Science and Technology, Kwansei Gakuin University, Sanda, Hyogo 669-1337, Japan

†Electronic supplementary information (ESI) available. See DOI: 10.1039/c7pp00449d





**Fig. 1** (a) Chemical structure of PtCP. (b) SEM image of the nano-porous glass. (c) Appearance of the PtCP-fixed porous glass.

porphyrin I (PtCP, Fig. 1a), a tetracarboxylic-acid derivative of Pt(II)-octaethylporphyrin (PtOEP), which is widely used as an oxygen sensor,<sup>1–3</sup> a red OLED pigment,<sup>6–8</sup> and a TTA-UC sensitizer.<sup>12–15</sup> For anionic carboxylic-acid groups, it is possible to bind chromophores to the surface of the nano-pore through ionic interaction after replacing silanol groups on the glass surface with cationic amino groups.<sup>21</sup> This hybrid material can be equipped with the various features discussed above such as strong absorption due to multiple interfaces along the optical path in the 3D-pore-network like bulk-heterojunctions in organic photovoltaic devices, high loading concentration and a possibility of monomeric dispersion due to the large surface area and free volumes, allowing the other materials to penetrate. We found that the chromophores can retain their monomeric nature in the hybrid and show superior properties to those in solution, namely higher phosphorescence quantum yield at higher loading concentration beyond solubility in solution. Phosphorescence lifetime measurements clarify that suppression of nonradiative deactivation due to the fixing of chromophores on the solid surface is a key to superior phosphorescence properties.

## Experimental

Nano-porous glass was prepared by a previously reported method.<sup>21</sup> Borosilicate glass with a composition of SiO<sub>2</sub>:62.5%-B<sub>2</sub>O<sub>3</sub>:28.3%-Na<sub>2</sub>O:9.2% in weight (Akagawa glass, 20 × 20 × 0.5 mm<sup>3</sup>) was cut into pieces (10 × 10 × 0.5 mm<sup>3</sup>), and then heated at 600 °C for 72 h in air to induce nanoscopic phase separation between SiO<sub>2</sub> and B<sub>2</sub>O<sub>3</sub> in each piece. The B<sub>2</sub>O<sub>3</sub> phase was leached from the glass by treatment with 0.5 mol l<sup>-1</sup> sulfuric acid at 99 °C for 96 h, followed by drying at 140 °C for 3 h under vacuum. The pore size distribution was carried out by mercury porosimetry<sup>22</sup> (Thermo Scientific Pascal 240) in the pressure range of 0 to 200 MPa. This is the method in which the intrusion of mercury into a porous sample as a function of the applied pressure is analyzed and gives more precise information than the nitrogen adsorption method in the pore range of several 10 nm.<sup>23</sup> The average diameter of the formed nano-pores was 55.6 nm and the surface area was 35.2 m<sup>2</sup> g<sup>-1</sup>. The nano-porous glass was then refluxed with 3-aminopropyltrimethoxysilane as a coupling agent and rinsed in toluene at 99 °C for 3 h. PtCP ((3,8,13,18-tetramethylporphyrin-2,7,12,17-tetrapropionato)platinum(II),

Frontier Scientific C40425) was used without further purification. To fix PtCP on the surface of the nano-porous glass, pieces of the glass were dipped in a PtCP solution (75 μM) in tetrahydrofuran (THF). In the cases where the loading concentration of PtCP was higher than 1 mM, the solution was additionally refluxed for 3 h. The loading concentration of PtCP was controlled by the dipping (and reflux) time. The glass pieces were then rinsed in THF at 60 °C for several hours to remove unreacted PtCP. Through this treatment, the surface area was reduced, but remained in the same order of magnitude as the original sample. This was followed by optical measurements of the PtCP-fixed porous glass.

UV-vis absorption spectra were recorded using a Shimadzu UV3150 spectrophotometer. The phosphorescence spectrum and quantum yield ( $\Phi_p$ ) were measured using a spectrometer combined with a calibrated integrating sphere (Hamamatsu Photonics, C9920)<sup>24</sup> under air or Ar (99.99% + ). Phosphorescence decay was measured with a custom setup using a frequency-doubled ns-Nd:YAG laser (532 nm, a pulse width of 20 ns, a repetition rate of 10–15 Hz) as the light source. The incident pulse energy was 11 μJ or as noted otherwise. A piece of the dye-fixed glass placed in a sealed glass tube under either Ar or vacuum was used as the sample. The emission from the sample was collected by using a lens and guided to a monochromator (Jobin-Yvon H-10) through an OD4 notch filter to block 532 nm scattering. The signal was detected using a photomultiplier (Hamamatsu R936) and recorded using a digital oscilloscope (500 MHz, 5 G<sub>s</sub> s<sup>-1</sup>).

All the optical measurements were performed at 23 °C.

## Results

### UV-vis absorption spectrum

The prepared porous glass contained 3D-continuous pores of nm-dimensions as seen in the scanning electron microscopy (SEM) image (Fig. 1b). The nano-porous glass before dye-fixing (blank) was snow-white due to light scattering, and pink after the PtCP was fixed (Fig. 1c). The UV-vis absorption spectrum of the blank porous glass showed a monotonic increase with decreasing wavelength, which is a characteristic feature of light scattering (Fig. 2a). On the other hand, the spectrum of PtCP-fixed porous glass showed a sharp peak overlapping the scattering spectrum. The differential spectrum showed a strong peak at 534 nm and a weak peak at 501 nm (Fig. 2b), assigned to the Q(0, 0) and Q(1, 0) bands, respectively, exactly matching the spectral shape and wavelength of PtCP in THF solution. Loading concentrations of PtCP in the nano-porous glass were calculated from the absorbance of the Q(0, 0) band, the thickness of the glass samples, and the molar absorption coefficient of the Q(0, 0) band ( $3.7 \times 10^4 \text{ M}^{-1} \text{ cm}^{-1}$  in THF).

As control experiments, (1) non-ionic Pt-porphyrin (Pt-octaethylporphyrin) was used instead of PtCP, and (2) the bare porous glass was treated by silanol coupling instead of amino coupling while keeping other conditions the same as before. Both control samples were snow-white and showed no absorp-





**Fig. 2** UV-vis absorption spectra of (a) PtCP-fixed porous glass with a concentration of 77  $\mu\text{M}$  (red line) and blank porous glass (dashed black line). (b) Normalized UV-vis absorption spectra of PtCP obtained by subtracting the blank porous glass from the PtCP-fixed porous glass (solid black line) and PtCP in THF with a concentration of 7.9  $\mu\text{M}$  (solid red line).

tion peaks at the  $Q(1,0)$  and  $Q(0,0)$  bands in their UV-vis absorption spectra as shown in Fig. S1 in the ESI.† These facts clearly show that PtCP was fixed by forming ionic bonds between carboxyl groups of PtCP and amino groups on the surface of the glass.

### Phosphorescence spectrum

Upon excitation with 532 nm near the  $Q(0,0)$  band, PtCP-fixed porous glass showed vivid deep red emission under an Ar atmosphere. The spectrum has a peak at around 649 nm and a shoulder at 713 nm (Fig. 3). Despite changing the loading concentration of PtCP from 75  $\mu\text{M}$  to 310  $\mu\text{M}$ , 5.1 mM, the spectral shape remained the same with a slightly red-shifted peak wavelength (2 nm) from that of PtCP in THF solution. It is worth noting that the spectra have no dimer emission peaks (770 nm).<sup>25</sup> From the good agreement in the spectral shape of the absorption and phosphorescence spectra between the PtCP-fixed porous glass samples and the solution, in addition to the absence of the dimer emission peaks for the glass sample, it can be concluded that most of the PtCP was molecularly dispersed on the surface of the nano-pore of the glass



**Fig. 3** Phosphorescence emission spectra of PtCP fixed in nanoporous glass with different loading concentrations of 75  $\mu\text{M}$  (blue), 310  $\mu\text{M}$  (green), and 5.2 mM (red) together with PtCP solution in THF (75  $\mu\text{M}$ , black). All samples were deoxygenated by Ar-bubbling.

without forming a considerable amount of aggregate. As PtCP cannot dissolve more than 300  $\mu\text{M}$  in THF solution, this material therefore contains a higher PtCP-loading concentration while being free of aggregation. Meanwhile, the shoulder at around 720 nm of the PtCP-fixed glass with 5.1 mM concentration was slightly higher than that of glass samples with lower concentration, indicating that there may be a few dimer-like components.

### Phosphorescence quantum yield

The phosphorescence quantum yield  $\Phi_p$  of the PtCP-fixed glass under an Ar atmosphere was found to be around 0.25 at a loading concentration of 75  $\mu\text{M}$ , though it fluctuated somewhat from sample to sample (Fig. 4). Interestingly, the observed  $\Phi_p$  of the PtCP-fixed samples were much higher than those in the same concentration of THF solution ( $0.16 \pm 0.018$ , shown with a triangle in Fig. 4). The  $\Phi_p$  of the PtCP-fixed glass remained constant or gradually decreased with an increase in loading concentration. However, even at the higher loading concentration of 0.64 mM, the value was higher than that of the solution at 75  $\mu\text{M}$ . Meanwhile, the  $\Phi_p$  at concentrations of 4.4 and 5.1 mM are reduced to about 0.1 probably due to self-quenching.<sup>26</sup> In contrast to the high  $\Phi_p$  under an Ar atmosphere, the phosphorescence of the glass samples was perfectly quenched ( $\Phi_p < 0.005$ ) in the presence of oxygen under the regular atmospheric conditions.<sup>27</sup> This suggests that oxygen can diffuse in porous glass through the continuous nano-pores.

### Phosphorescence lifetime

The phosphorescence of PtCP-fixed glass with 75  $\mu\text{M}$  concentration exhibits a single exponential decay ( $\tau = 95 \mu\text{s}$ , Fig. 5) under Ar conditions. The lifetime was unchanged after increasing the excitation intensity up to five times (data not shown). On the other hand, the decays became multi-exponential though the increase of the PtCP loading concentration and were analysed with a double-exponential function (Fig. 5 and



**Fig. 4** Phosphorescence quantum yield of PtCP-fixed glass as a function of PtCP concentration in air (black circle) and under an Ar atmosphere (red square). The green triangle shows that of a PtCP solution in THF with a concentration of 75  $\mu\text{M}$  under an Ar atmosphere.



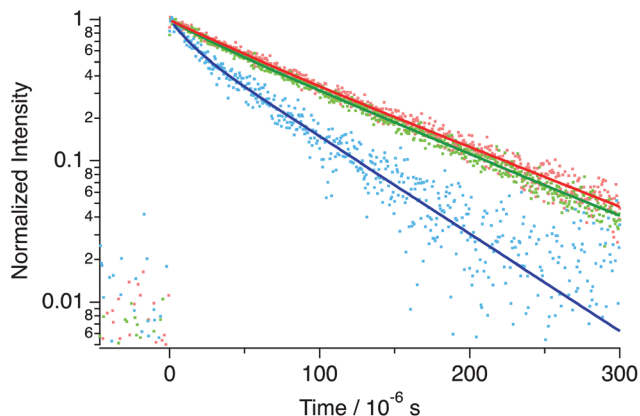


**Fig. 5** Phosphorescence decay of PtCP-fixed glass with different loading concentrations of PtCP: 75  $\mu\text{M}$  (red), 310  $\mu\text{M}$  (green), and 5.1 mM (blue) measured under an Ar-atmosphere with their curve fit (solid lines of the corresponding colors) to single- (75  $\mu\text{M}$ ) and double-exponential (310  $\mu\text{M}$  and 5.1 mM) functions.

Table 1). At a loading concentration of 310  $\mu\text{M}$ , a fast component with a lifetime of 25  $\mu\text{s}$  appeared while the lifetime of the slow component remained unchanged. The relative amplitude of the fast component was small (12%) and the shape of the decay was similar to that of 75  $\mu\text{M}$ . At 5.1 mM, lifetimes of both the fast and slow components were shorter than that of 75  $\mu\text{M}$  and the relative amplitude of the fast component increased (28%). We also measured the lifetime in the presence of oxygen with several concentrations (0.4–21% in volume for the 75  $\mu\text{M}$  sample). The lifetime decreased with an increase in concentration (Fig. S2 in the ESI†).

Interestingly, these lifetimes were longer than those of the solution. At the same PtCP concentration of 75  $\mu\text{M}$ , the PtCP-fixed glass had a phosphorescence lifetime twice that of the THF solution (48  $\mu\text{s}$  and 25  $\mu\text{s}$  for the Ar-bubbled sample and  $48 \pm 1 \mu\text{s}$  for the freeze-pump-thaw degassed sample, Fig. 6).

Radiative and nonradiative rate constants ( $k_r$  and  $k_{nr}$ , respectively) were estimated from the obtained lifetimes,  $\tau$ , and  $\Phi_p$  using the following equations:  $k_r = \Phi_p \tau^{-1}$  and  $k_{nr} = \tau^{-1} - k_r$ , assuming that the quantum yield of intersystem crossing of PtCP was unity.<sup>28</sup> It was found that the  $k_{nr}$  of PtCP on the surface of the nano-porous glass was less than half of that in solution (THF) while the  $k_r$  were almost the same (Table 1),



**Fig. 6** Phosphorescence decays of PtCP-fixed glass (red) and PtCP solutions in THF deoxygenated by Ar bubbling (green) and by freeze-pump-thaw cycles (orange), together with fitting curves (solid lines, see text). The concentration of PtCP was 75  $\mu\text{M}$  for all samples. The excitation energy was 7.3  $\mu\text{J}$  per pulse.

suggesting that the nonradiative deactivation pathway was suppressed when the dye molecule was fixed on the solid surface.

Meanwhile, comparison of the PtCP-fixed porous glass samples shows decreasing  $k_r$  and increasing  $k_{nr}$  as the PtCP loading concentration increased. We used the average lifetime defined as  $\langle \tau \rangle = \sum_i \tau_i^2 A_i / \sum_i \tau_i A_i$  (where  $A_i$  is the relative amplitude)<sup>29</sup> for the 310  $\mu\text{M}$  and 5.1 mM samples to obtain  $k_r$  and  $k_{nr}$  as their phosphorescence decays were multi-exponential. The use of average lifetime blurs the theoretical basis for the estimation of  $k_r$  and  $k_{nr}$ ; nevertheless, they indicate the general tendency of acceleration and suppression of radiative and non-radiative decays, respectively, at high loading concentration.

## Discussion

To understand the spectroscopic properties of PtCP-fixed on the surface of nano-porous glass, we consider the intermolecular distance of two neighboring PtCP molecules,  $d$ , from the loading concentration and the surface area of the nano-porous glass (Table 1). For the solution,  $d$  was calculated from the inverse cubic root of the number density of molecules. The  $d$  for the 75  $\mu\text{M}$  porous glass (27 nm) was the same as that of the solution with the same concentration (28 nm), suggesting that each PtCP molecule on the glass surface has

**Table 1** Quantum yield, lifetimes, and rate constants of phosphorescence of the PtCP-fixed nano-porous glass and the solution, and the average distance between PtCP molecules

Sample	$\Phi_p$	$\tau_1/\mu\text{s}$ ( $A_1$ )	$\tau_2/\mu\text{s}$ ( $A_2$ )	$\langle \tau \rangle/\mu\text{s}$	$k_r/10^3 \text{ s}^{-1}$	$k_{nr}/10^3 \text{ s}^{-1}$	$d/\text{nm}$
Porous glass	75 $\mu\text{M}$	0.29	$95 \pm 1$	—	—	3.1	7.5
	310 $\mu\text{M}$	0.21	$96 \pm 2$ (0.88)	$25 \pm 1$ (0.12)	$94 \pm 2$	2.2	8.4
	5.1 mM	0.08	$63 \pm 1$ (0.72)	$11 \pm 1$ (0.28)	$59 \pm 2$	1.4	15
THF (under Ar atmosphere)	75 $\mu\text{M}$	0.16	$48 \pm 1$ (0.74)	$25 \pm 1$ (0.26)	$45 \pm 1$	3.6	19
							28

$\Phi_p$  is the phosphorescence quantum yield.  $\tau_i$  and  $A_i$  are the lifetime and relative amplitude ( $i = 1, 2$ ) of PtCP phosphorescence, respectively.  $\langle \tau \rangle$  is the average lifetime for the double-component decays.  $k_r$  and  $k_{nr}$  are radiative and nonradiative rate constants of PtCP triplet excited states (the average lifetime was used to calculate the double-component decays).  $d$  is the average distance between PtCP molecules on the surface for the PtCP-fixed glass calculated from the surface area and volume for the PtCP solution calculated from the concentration.



enough space between neighbors to be dispersed on a molecular level as the size of each molecule is around 2 nm (Fig. 1a). This supports the observation that the absorption and phosphorescence spectra are identical to those of the solution and PtCP is fixed while maintaining molecular dispersion. Moreover, the smaller  $k_{nr}$  obtained from the higher  $\Phi_p$  and the longer  $\tau$  – compared to the solution – indicates a suppressed deactivation pathway on the glass surface. The binding of the molecule to the surface by ionic interaction could be a possible cause of suppression from the restricted freedom of motion on the surface.

The increase of loading concentration reduced  $d$  to 16 nm for 310  $\mu\text{M}$  and 2.9 nm for 5.1 mM. At 310  $\mu\text{M}$ , each molecule has significant intermolecular distance relative to its size, while at 5.1 mM they are comparable, thus allowing the neighboring molecules to contact and form aggregates. This scenario agrees with the observation that  $\Phi_p$  and  $\tau$  of the 310  $\mu\text{M}$  sample were almost identical to those of the 75  $\mu\text{M}$  sample while decreasing  $\Phi_p$  and decreasing  $\tau$  were observed for the 5.1 mM sample. The decreasing lifetime implies the existence of aggregation,<sup>27</sup> which can enhance  $k_{nr}$  through mechanisms such as intermolecular vibration.

## Conclusions

Through the use of ionic bonds, we successfully fabricated PtCP fixed nano-porous glass in which PtCP is molecularly dispersed on the surface of a 3D-network of nano-pores. It is worth noting that the phosphorescence quantum yield and loading concentration are much higher than the limits of PtCP in solution. The molecular dispersion of PtCP at 75 and 310  $\mu\text{M}$  loading concentration was demonstrated by monomeric absorption and phosphorescence spectra and supported by the estimated intermolecular distance on the surface. This is consistent with the constant and high quantum yield ( $\Phi_p \sim 25\%$ ) at these loading concentrations. The phosphorescence lifetime measurements clarified that PtCP bonded on glass surface has a much longer lifetime than that in inert solvent, facilitating the high  $\Phi_p$  by suppressing nonradiative deactivation pathways likely a result of the limited freedom of molecular motion from bonding to the nano-porous surface.

At high loading levels of the order of 5 mM, it was found that  $\Phi_p$  dropped with the lifetime, since the loading concentration is nearly saturated as the intermolecular distance approaches the size of the molecule. The molecular dispersion on the surface was considered to be disrupted by the high density of molecules.

The present results reveal that PtCP fixed on a nano-pore surface has unique properties differing from those in solution, and shows superior performance as a phosphorescent material for device applications. The through-hole network of nano-pores allows the flow or storage of gases, liquids and solids, which can be applied to oxygen sensors, wavelength-conversion devices based on the TTA-UC mechanism, and other

devices. An application study for TTA-UC devices is currently in progress in our lab.

## Conflicts of interest

There are no conflicts to declare.

## Acknowledgements

This work was supported by JSPS KAKENHI Grant Numbers JP26107004 and JP17K05852 in Scientific Research on Innovative Areas “Photosynergetics” and in Scientific Research (C), respectively. We thank Dr Takeyuki Uchida of Innovation-Boosting Equipment Common (IBEC), AIST, for the SEM observation. We also thank Ms Yuuko Matsumoto of IFMRI for the fabrication of nano-porous glass and PtCP-fixed glass. Furthermore, we thank Dr Hiroaki Sakurai and Ms Masako Iwamatsu for the gas chromatography measurements.

## Notes and references

- 1 D. B. Papkovsky, J. Olah, I. V. Troyanovsky, N. A. Sadovsky, V. D. Rumyantseva, A. F. Mironov, A. I. Yaropolov and A. P. Savitsky, *Biosens. Bioelectron.*, 1992, **7**, 199.
- 2 Y. Amao, K. Asai, T. Miyashita and I. Okura, *Chem. Lett.*, 1999, **10**, 1031.
- 3 B. Zelelow, G. E. Khalil, G. Phelan, B. Carlson, M. Gouterman, J. B. Callis and L. R. Dalton, *Sens. Actuators, B*, 2003, **96**, 304.
- 4 C.-J. Jin and J.-W. Park, *Sens. Actuators, B*, 2017, **253**, 934.
- 5 C.-S. Chu and T.-H. Lin, *Sens. Actuators, B*, 2014, **202**, 508.
- 6 S. Lamansky, R. C. Kwong, M. Nugent, P. I. Djurovich and M. E. Thompson, *Org. Electron.*, 2001, **2**, 53.
- 7 E. M. Gross, N. R. Armstrong and R. M. Wightman, *J. Electrochem. Soc.*, 2002, **149**(5), E137.
- 8 T. Tsuboi, Y. Wasai and N. Nabatova-Gabain, *Thin Solid Films*, 2006, **496**, 674.
- 9 M. Janghouri, *J. Electron. Mater.*, 2017, **46**, 5635.
- 10 M. Janghouri and M. Adinech, *J. Photochem. Photobiol., A*, 2017, **341**, 31.
- 11 M. R. Jafari and B. Bahrami, *Appl. Phys. A*, 2015, **119**, 1491.
- 12 A. Monguzzi, R. Tubino, S. Hoseinkhani, M. Campione and F. Meinardi, *Phys. Chem. Chem. Phys.*, 2012, **14**, 4322.
- 13 N. Yanai and N. Kimizuka, *Chem. Commun.*, 2016, **52**, 5354.
- 14 K. Kamada, Y. Sakagami, T. Mizokuro, Y. Fujiwara, K. Kobayashi, K. Narushima, S. Hirata and M. Vacha, *Mater. Horiz.*, 2017, **4**, 83.
- 15 Q. Dou, L. Jiang, D. Kai, C. Owh and X. J. Loh, *Drug Discovery Today*, 2017, **22**, 1400.
- 16 Y. Bai, J.-H. Olivier, H. Yoo, N. F. Polizzi, J. Park, J. Rawson and M. J. Therien, *J. Am. Chem. Soc.*, 2017, **139**, 16946.
- 17 V. Gray, K. Börjesson, D. Dzebo, M. Abrahamsson, B. Albinsson and K. M. Poulsen, *J. Phys. Chem. C*, 2016, **120**, 19018.



- 18 S. Takagi, T. Shimada, M. Eguchi, T. Yui, H. Yoshida, D. A. Tryk and H. Inoue, *Langmuir*, 2002, **18**, 2265.
- 19 S. Takagi, M. Eguchi, D. A. Tryk and H. Inoue, *J. Photochem. Photobiol., C*, 2006, **7**, 104.
- 20 T. Tanaka, T. Yazawa, K. Eguchi, H. Nagasawa, N. Matsuda and T. Einishi, *J. Non-Cryst. Solids*, 1984, **65**, 301.
- 21 T. Jin, A. H. Ali and T. Yazawa, *Chem. Commun.*, 2001, 99.
- 22 W. D. Kingery, H. K. Bowen and D. R. Uhlmann, *Introduction to Ceramics*, Wiley, New York, 2nd edn, 1976, p. 425.
- 23 H. Giesche, *Part. Part. Syst. Charact.*, 2006, **23**, 1.
- 24 K. Suzuki, A. Kobayashi, S. Kaneko, K. Takehira, T. Yoshihara, H. Ishida, Y. Shiina, S. Oishi and S. Tobita, *Phys. Chem. Chem. Phys.*, 2009, **11**, 9850.
- 25 H. Goudarzi and P. E. Keivanidis, *J. Phys. Chem. C*, 2014, **118**, 14256.
- 26 A. K. Bansal, W. Holzer, A. Penzkofer and T. Tsuboi, *Chem. Phys.*, 2006, **330**, 118.
- 27 J. R. Lakowicz, *Principles of Fluorescence Spectroscopy*, Springer, New York, 3rd edn, 2006, p. 317.
- 28 The quantum yield of intersystem crossing of Pt-octaethylporphyrin (i.e., replaced carboxylic acid with ethyl group in PtCP) was reported to be 0.9 in J. Kavandi, J. Callis, M. Gouterman, G. Khalil, D. Wright and E. Green, *Rev. Sci. Instrum.*, 1990, **61**, 3340.
- 29 J. R. Lakowicz, *Principles of Fluorescence Spectroscopy*, Springer, New York, 3rd edn, 2006, p. 142.

